DOI: 10.1021/ma1005777

Macromolecules
ARTICLE

Micropatterns of Hierarchical Self-Assembled Block Copolymer Droplets with Solvent-Assisted Wetting of Brush Monolayers

Tae Hee Kim, June Huh, and Cheolmin Park*

Department of Materials Science and Engineering, Yonsei University, Seoul 120-749, Korea

Received March 16, 2010; Revised Manuscript Received May 7, 2010

ABSTRACT: We present a method to fabricate micropatterns of a self-assembled block copolymer droplets with hierarchically ordered nanostructures by controlling solvent-assisted wetting of the droplets. This method is based on transfer-printing the micropatterned dewetted droplets formed onto a topographic poly(dimethylsiloxane) prepattern to a silicon wafer, followed by wetting triggered by solvent annealing. Solvent vapor provides sufficient mobility of block copolymer molecules in convex-shaped micropatterns and allows for controlling the 2D circular spread of the ~7 nm thick brush monolayer, resulting in a novel structure hierarchically terraced with ordered spherical microdomains in the individual block copolymer droplets. Our micropatterning technique capable of controlling both shape and microstructure of individual droplets also enables us to produce a novel polarity tunable surface since contact angle of a water droplet is easily tailored as a function of solvent annealing time on micropatterns.

Introduction

Hierarchical structures evolved from nanometer, micrometer to millimeter scale with periodic orders have been successfully driven by self-assembly of block copolymers in virtue of their diverse structural motifs and at the same time facile tunability of the structures.[1−3] The simple and cost-effective characteristics of the block copolymers have drawn many emerging applications in nanotechnology such as nanolithography, photonic crystals, nanotemplates for harvesting metals and semiconductors, and drug carriers.[1−4] In particular, surface wetting and/or dewetting of thin block copolymer films have been often utilized as an effective route for fabricating interesting hierarchical structures.[5−10]

The spreading of nonvolatile liquid droplets on a wettable substrate has been in fact a long-standing issue attracting much interest due to its implications for understanding lubrication, molecular scale friction, and coating and thus for controlling hard surfaces.[11−15] The spreading frequently accompanies the formation of unique molecular and/or nanometer scale terraces characterized by distinct monomolecular layers in the direction of z normal to the surface.[16−21] When a self-assembled material with an ordered structure, on a molecular or nanometer level, is employed for wetting on a hard surface, the system becomes more complicated, and therefore, one should take into account not only the first layered terrace directly on the solid surface, frequently known as a frontier layer, but also multiple terraces regularly spaced in the z-direction arising from the ordered structure.[16−21] There have been several theoretical[16−18] and experimental studies[19−21] dealing with the dynamics of terraced droplets of structured fluids such as smectic liquid crystals and block copolymers.

Block copolymers with lamellar microstructures showed very unique terraced hierarchical structures formed upon either dewetting a thin homogeneous film or wetting a distinct droplet.[6−9] Disklike concentric rings with the characteristic periodicity of the block copolymer were for instance successively piled up in the droplet whose cross section resembles a triangle with a stepped side profile.[7,9] In this case, the monolayered first terrace was evenly formed on a substrate frequently called the brush monolayer of a block copolymer, in which one of the blocks is preferential to the surface with the other nonpreferential block pointing toward the air.[7]

The regularly spaced wetting and/or dewetting of a structured fluid in the z-direction is no doubt useful for understanding the origin and dynamics of the structural formation; however, there are several issues that require consideration for utilizing it in further applications. The droplets that have been investigated so far are all varied in size from micrometers to millimeters. Narrowly distributed micrometer- or submicrometer-scale droplets would potentially provide interesting micropatterning applications such as self-cleaning surfaces,[22] biochemical sensors,[23] and microlens arrays.[24,25] It would be very desirable, therefore, to develop a way that allows to control all x-, y-, and z-directions, whereby one could imagine nearly monodispersed microdroplets terraced in a z-direction and at the same time arrayed on the xy-plane in a periodic order. Such a system would also offer a more convenient route for investigating the growth of brush monolayers in a controlled manner.

In the present study, we have achieved the micropatterns of the terraced block copolymer microdroplets based on transfer-printing the microdroplets periodically dewetted on a topographic poly(dimethylsiloxane) (PDMS) prepattern onto a hard substrate and subsequently solvent annealing them.[26−29] Solvent vapor treatment gives rise to the wetting of the patterned droplets, initiated with the concentric spreading of the characteristic brush monolayer, and thus allows for precise monitoring of the growth of the brush monolayer over time. The method presented here enables the fabrication of patterned arrays of the multiterraced microdroplets which consist of both brush monolayer and hierarchically ordered block copolymer microdomains over a large area. Our micropattern also becomes a water contact angle tunable surface in which precise control of the wetting of both brush monolayer and microdroplet with solvent annealing time allowed for tailoring macroscopic surface polarity of a substrate with the arrays of the block copolymer droplets.

*Corresponding author: Tel +82-2-2123-2833; Fax +82-2-312-5375; e-mail cmpark@yonsei.ac.kr.

 Published on Web 05/19/2010 © 2010 American Chemical Society

Experimental Section

Materials. A PS-*b*-PEO block copolymer with a total molecular weight of 26 500 g/mol and a polydispersity of 1.06 was purchased from Polymer Source, Inc. (Doval, Canada). The molecular weights of PS and PEO are 20 000 and 6500 g/mol, respectively, corresponding to a 22% minority block volume fraction. In bulk, the block copolymer was self-organized into hexagonally packed PEO cylindrical microdomains embedded in a PS matrix. 2 wt % PS-*b*-PEO solutions were prepared in benzene.

Micropatterning. An elastomeric PDMS mold was fabricated by curing a PDMS precursor (Sylgard 184, Dow Corning Corp.) on a prepatterned silicon master. We used a mixture of PDMS precursor and curing agent (10:1 by weight) that had been degassed under vacuum. The prepatterned photoresist masters were prepared by standard photolithography, and the surface of a master was fluorinated before casting the PDMS precursor on the master. After the PDMS precursor was cured at 60 °C for 6 h using vacuum oven, the mold was separated from the master. The PDMS molds with hexagons arrayed into hexagonal *p6mm* symmetry have several hexagon sizes ranging from 10 to 40 μm. In addition, a 2-dimensional PDMS mold was prepared with 20 μm squares arrayed into tetragonal symmetry. A 1-dimensional line pattern was also made of 20 μm in width.

Microarrayed convex lens-shaped spherical caps of dewetted droplets of the PS-*b*-PEO were developed on a patterned PDMS mold via spin-casting (SPIN 1200 Midas-system, Korea) at 2000 rpm and directly transferred to the Si substrates using different surface energies. The transfer of the PS-*b*-PEO film onto a substrate was performed using conformal contact with gentle pressure for 1 min. The removal of the PDMS pattern after the conformal contact produced patterned PS-*b*-PEO droplets on the Si substrate at room temperature without the application of additional heat. In order to control the surface polarity of a PDMS pattern, oxygen plasma treatment was performed for various time with the power of 40 W (PDC-32G Harrick Plasma).

Solvent Annealing. Microarrayed droplets of the PS-*b*-PEO on a Si substrate were placed in a chamber with a mixture of saturated water (vapor pressure at 25 °C: 24 mmHg) and benzene vapor (vapor pressure at 25 °C: 95 mmHg) for various solvent annealing times (10 s−48 h). The environment outside the chamber was maintained at 25 °C and 20% humidity. The films were removed from the chamber at set observation times.

Characterization. The morphologies of microarrayed droplets and their nanostructures were observed using a tapping mode atomic force microscope (AFM) (Nanoscope IV[a] Digital Instruments) in height and phase contrast and an optical microscope (OM) (Olympus BX 51M) in bright field. Contact angle measurement was performed with contact angle meter (CAM101 model, KSV Instruments Ltd., Finland).

Results and Discussion

A poly(styrene-*block*-ethylene oxide) (PS-*b*-PEO) copolymer was employed for fabricating patterned arrays of the microdroplets onto a topographic PDMS prepattern as shown in the schematic of Figure 1. The dewetting occurred preferentially on the individual mesas when a PS-*b*-PEO solution was spin-coated onto a PDMS prepattern. Dewetted domains, each of which forms a spherical cap, are located near the center regions of the 20 μm hexagonal mesas arrayed with *p6mm* hexagonal symmetry with the periodicity of 30 μm while trench regions are completely filled with the block copolymer film as shown in Figure 2a. The height profile of a microdroplet on the hexagonal prepattern from an AFM image in the inset of Figure 2a also revealed the diameter and the maximum height of the droplet of approximately 6 μm and 600 nm, respectively.

The dewetting is initiated at the sharp edge of topographic patterns due to localized polymer flow at the pattern edges in order to spontaneously reduce the excess chemical potential induced by

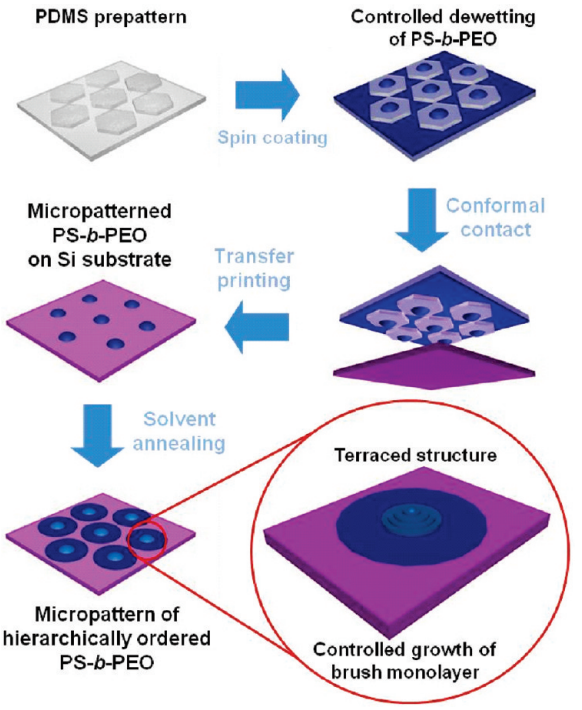

Figure 1. Procedure for controlling the growth of brush monolayers of micropatterned arrays of hierarchically ordered PS-*b*-PEO droplets on a solid substrate. The dewetting of the film on hexagonal patterned PDMS molds is selectively confined to the center of the mesa regions, and subsequent transfer printing to Si substrate gives rise to patterned PS-*b*-PEO droplets. Solvent annealing provides sufficient mobility for the block copolymer molecules in convex-shaped patterned domains and allows control of the 2D circular spread of brush monolayers of the block copolymer, which leads to a hierarchical terraced structure with ordered microdomains.

high curvature at the pattern edge, which causes draining of fluid from the mesas to the trenches.[30] Similar dewetting patterns have been observed in spin-coated polymer on the topographic pattern.[31,32] The capillary-driven flow will rapidly tend to raise the thickness of the solution in the trenches, thus reducing the curvature difference and the capillary pressure. This planarization of the film on a topographic surface renders the film on mesa regions thinner than on trenches. The planarization is proportional to surface tension and inversely proportional to both viscosity and shrinking speed with a parameter of ratio [(surface tension)/{(viscosity) × (shrinking speed)}].[31,32] Further planarization can give rise to an incomplete wetting of the thinner film on the elevated mesa regions, leading to block copolymer droplets, each on the center of the individual mesas, as shown in Figure 2a.

The wettability of thin PS-*b*-PEO films was thus simply controlled by the surface polarity of a PDMS pattern by an oxygen plasma treatment. We monitored the microdroplet formation on a PDMS pattern with oxygen plasma time. The droplets are apparently flattened out on individual mesas when the polarity of the PDMS pattern was enhanced by oxygen plasma, as shown in Figure 2. When the PDMS prepattern was exposed for only 7 s at 40 W, partially dewetted PS-*b*-PEO films were formed over the mesa area in Figure 2b. On the other hand, the plasma treatment for 15 s in our experimental setup for instance resulted in PS-*b*-PEO films completely wetted over all the mesa area (Figure 2e). A plot shown in Figure 2f exhibits the surface coverage of PS-*b*-PEO on a mesa as a function of oxygen plasma time.

The size of convex lens shaped, spherical caps of a dewetted droplet was varied by changing the size of the PDMS hexagons. As the size of the PDMS hexagon decreases, the size of the spherical cap does as well. The droplets are ~2 μm in diameter on

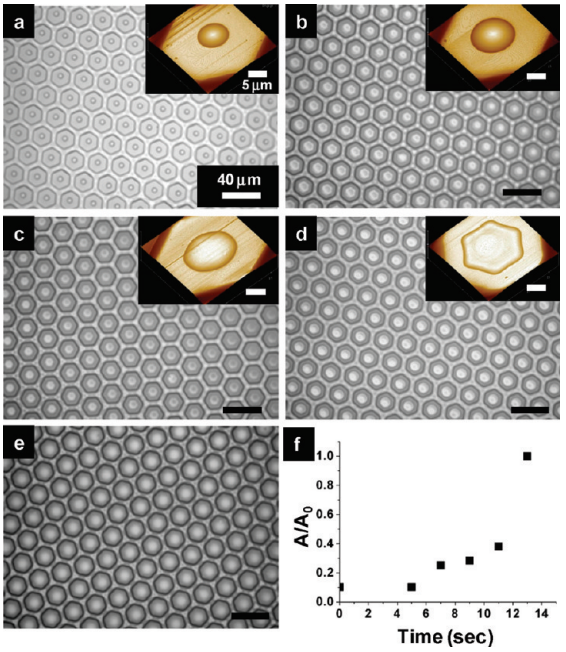

Figure 2. (a−e) OM images of arrays of PS-*b*-PEO dewetted droplets on a 20 μm hexagonal PDMS pattern whose surface polarity was controlled by an oxygen plasma treatment with different time intervals: (a) 0, (b) 7, (c) 9, (d) 11, and (e) 13 s. Water contact angles on a plasma-treated PDMS pattern were varied from 108°, 98°, 90°, 84° to 72° with the time intervals of 0, 7, 9, 11, and 13 s, respectively. (g) A plot of the ratio of the covered area by a droplet (A) to original hexagon area (A_0) as a function of the oxygen plasma treatment time. Insets of (a−d) are AFM images of individual droplets dewetted on hexagonal patterns after different oxygen plasma treatment.

the 10 μm PDMS hexagonal patterns, as shown in Figure 3a. Arrayed microdroplets with ~10 and ~7 μm in diameter were formed on 20 μm squares arrayed with 4*mm* symmetry and 1D periodic PDMS lines, respectively, as shown in Figure 3b,c. The observations thus far apply in principle to PDMS prepatterns of various shapes and sizes. An AFM image of a magnified droplet on a PDMS hexagon prepattern in Figure 3d shows that on the surface of a spherical-cap shaped droplet randomly ordered cylindrical PEO microdomains are embedded in PS matrix with an average diameter of 15 nm and center-to-center spacing of 30 nm, respectively. The rapid evaporation of benzene solvent in a block copolymer solution during spin-coating made films kinetically trapped, resulting in poorly ordered microdomains of the films.

The arrayed PS-*b*-PEO droplets dewetted on a PDMS prepattern were directly transferred onto a flat Si substrate with high transfer fidelity over 80%. The transfer was facilitated by conformal contact of PDMS mesas containing the dewetted droplets and a Si substrate for 1 min without additional heat and pressure. Figure 4a,b clearly exhibits the dewetted droplets transferred from ones on 20 μm PDMS hexagons in Figure 2a. In magnified OM and AFM images, as shown in Figure 4b,c, the diameter and height of the transferred droplet domain are about 6 μm and 600 nm, respectively, which correspond to those of the dewetted domains before transfer. On the surface of individually transferred droplets upside-down from the previous droplets on a PDMS, we also confirm that randomly ordered cylindrical PEO microdomains are embedded in PS matrix with an average diameter of 15 nm and center-to-center spacing of 30 nm, respectively (Figure 4d).

The pattern transfer in thin films from one layer to another is mainly governed by the difference in work of adhesion (T) involved with the surface tension of each layer. The work of adhesion

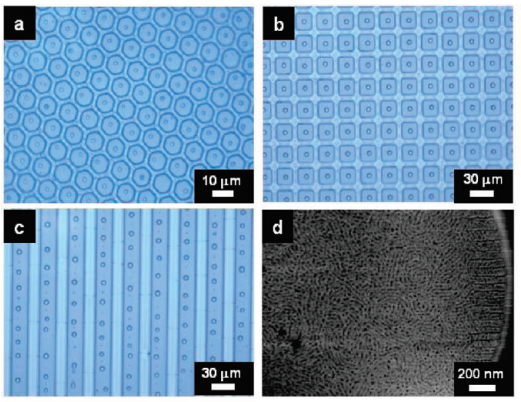

Figure 3. OM (a−c) and AFM (d) images of the microarryays of PS-*b*-PEO dewetted droplets on PDMS prepatterns. Microdroplets on (a) 10 μm PDMS hexagonal prepattern, 20 μm PDMS (b) square, and (c) line prepattern. (d) Surface nanostructure of a dewetted droplet on a 20 μm PDMS hexagonal prepattern in the phase mode. Randomly ordered cylindrical PEO microdomains are embedded in PS matrix.

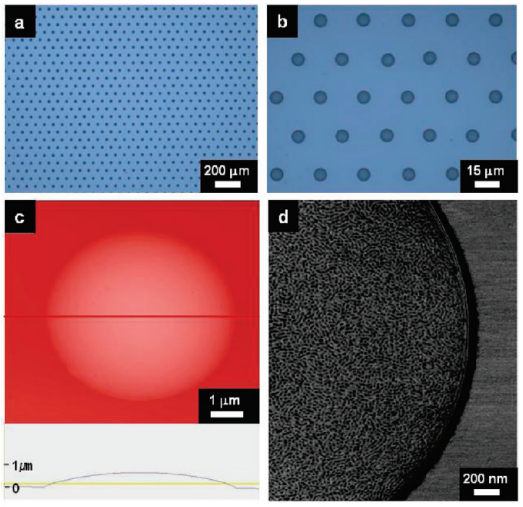

Figure 4. OM (a, b) and AFM (c, d) images of the microarrayed PS-*b*-PEO droplets on Si substrate after transfer printing. (a) Transferred PS-*b*-PEO droplets with the diameter of ~6 μm microarrayed with *p6mm* hexagonal symmetry. (b) A magnified OM image of (a). (c) (upper) Surface morphology of an individual droplet in height mode. (lower) A height profile of the droplet. (d) Surface nanostructure of an individual droplet clearly displays in-plane cylindrical PEO microdomains embedded in PS matrix.

at the PDMS mold and PS-*b*-PEO interface ($W_{\text{PDMS/PS-}b\text{-PEO}}$) should be less than that at the PS-*b*-PEO and substrate interface ($W_{\text{PS-}b\text{-PEO/SUB}}$), i.e., $T(= W_{\text{PS-}b\text{-PEO/SUB}} - W_{\text{PDMS/PS-}b\text{-PEO}}) > 0$ for successful transfer. The work of adhesion at layer 1 and 2 is generally given by[33,34]

$$W_{12} = 4\left(\frac{\gamma_1^d\gamma_2^d}{\gamma_1^d+\gamma_2^d} + \frac{\gamma_1^p\gamma_2^p}{\gamma_1^p+\gamma_2^p}\right)$$

where γ^p and γ^d correspond to polar and dispersion component of overall surface tension ($\gamma = \gamma^p + \gamma^d$), respectively. Since the droplet transfer occurred before solvent annealing, it is reasonable to take the surface energy value of an *as-cast* film. The surface tension of PS-*b*-PEO used in the current work was calculated from the geometric-mean method based on the equation of $(1 + \cos\theta_t)\gamma_t = 2\{(\gamma_t^d\gamma_s^d)^{1/2} + (\gamma_t^p\gamma_s^p)^{1/2}\}$,[27] where θ is contact angle of a testing liquid on PS-*b*-PEO surface and γ_t and γ_s are surface energy of testing liquid and solid surface. Water and ethylene

glycol were used as testing liquids at least required for the calculation of $\gamma^p_{PS\text{-}b\text{-}PEO}$ and $\gamma^d_{PS\text{-}b\text{-}PEO}$. On the basis of the contact angles of 80° and 70° for water and ethylene glycol on a thin *as-cast* PS-*b*-PEO film surface, $\gamma^p_{PS\text{-}b\text{-}PEO}$ and $\gamma^d_{PS\text{-}b\text{-}PEO}$ were obtained of 5.8 and 19.4 mJ/m^2, respectively. The computed values of $W_{PS\text{-}b\text{-}PEO/Si\ wafer}$ and $W_{PDMS/PS\text{-}b\text{-}PEO}$ are 67.0 and 41.2 mJ/m^2, respectively, which gives $T = 25.8$ mJ/m^2. This rationalizes the successful pattern transfer, consistent with our experimental results in Figure 4. It should be also noted that the contact area of a droplet on a PDMS is different from that on a Si surface due to the curved top surface of a droplet. The ratio of height to diameter of a droplet is, however, very small (~0.1), which allows us to ignore the surface area difference during transfer. In addition, a gentle pressure applied during conformal contact may minimize the contact surface area difference.

We have investigated how the transferred PS-*b*-PEO droplets are modified on a Si substrate during solvent annealing. It is apparent that the dewetted droplets transferred from PDMS surface spread out on Si substrate, making their diameter larger and larger with solvent annealing time. The captured morphologies of the sample after 3 min solvent treatment exhibit two distinct features as shown in Figure 5a,b. One is the formation of unique terraced structure on each droplet, and the other is the concentric growth of a thin sublayer around each droplet.

Upon spreading of a dewetted droplet on Si substrate, the characteristic terraced structure was developed, arising from the self-assembled microstructure of PS-*b*-PEO copolymer. The similar terraced structures have been reported in lamellar forming poly(styrene-*block*-methyl methacrylate) copolymers when the droplets were thermally annealed at a temperature above the glass transition temperatures of the consistent blocks and below order−disorder transition temperature (T_{ODT}) of the block copolymer.[7] Whereas, droplets thermally annealed above T_{ODT} showed typical smooth surface profiles similar to those obtained from homopolymers. Step height of the terraced droplet, therefore, corresponds precisely to lamellae periodicity of the block copolymer. In our micropatterned, terraced droplets, the step is ~20 nm in height as shown in the cross-sectional profile of Figure 5b. The terraced structure was also developed in the arrays of the smaller droplets of 5 μm in diameter after solvent annealing, as shown in Figure 5c. The observation of the surface of terraced droplets revealed circular PEO microdomains of ~20 nm in diameter well developed with improved ordering as compared to those observed in *as-transferred* droplets (Figure 5d).

In our system with the microarrays of the terraced droplets consisting of hexagonally ordered PEO microdomains, several implications should be made. First of all, the terraced structure developed upon solvent annealing implies that the improved ordering of PEO microdomains occurred through rearrangement or reorganization of the pre-existing PEO cylinders in *as-transferred* droplets without complete disordering of the structure. Second, the previous cylindrical PEO microdomains were transformed into spherical ones during solvent annealing. If the cylindrical PEO microdomains were aligned perpendicular to the surface as speculated from Figure 5d, the terraced structure with the step height of 20 nm would not be formed because the perpendicular cylinders do not require commensuration in *z*-direction. Our previous results have also demonstrated the cylinder-to-sphere transformation of PEO microdomains of the same block copolymer upon solvent annealing in the confined geometry.[5] With help of the detailed studies by Kramer et al.[35,36] of spherical morphologies developed by solvent annealing, two possible reasons were suggested: the selective swelling of PS blocks with benzene vapor in an individually isolated micropatterned film and the packing frustration of PEO cylinders in a spherical cap.[5] Both can be also affected to the current system and our results indeed confirm the order-to-order structural transition to spherical microdomains.

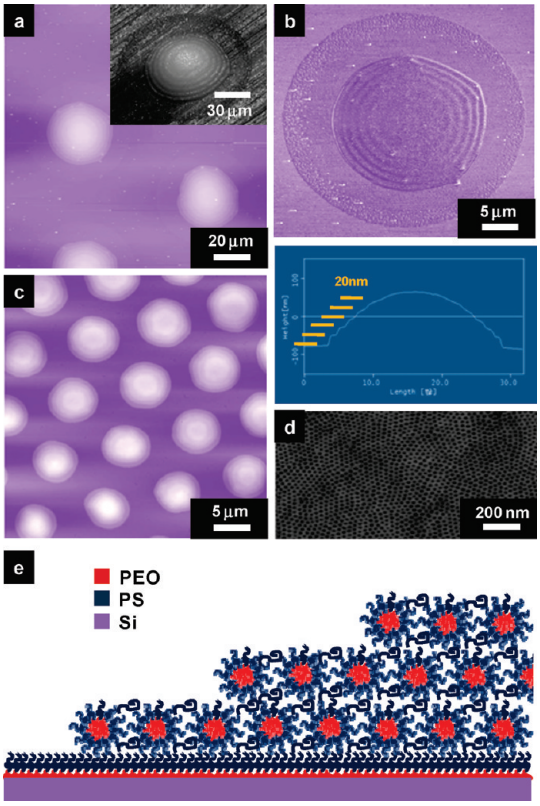

Figure 5. AFM images (a−d) of micropatterns of hierarchically terraced PS-*b*-PEO droplets with the concentric spreading of characteristic brush monolayers after solvent annealing. (a) Terraced PS-*b*-PEO droplets transferred with 40 μm hexagonal prepatterns. The inset shows a magnified image of a terraced droplet in 3-D visualization. Solvent vapor treatment time was about 170 s. (b) (upper) Terraced structure of an individual droplet with the 2D concentric spread of a brush monolayer of the block copolymer. (lower) A height profile of the droplet with ~20 nm in step height, corresponding to the size of the block copolymer microdomains. (c) Microarrayed and terraced PS-*b*-PEO droplets transferred with 10 μm hexagonal prepatterns. Solvent vapor treatment time was about 60 s. (d) Well-ordered PS-*b*-PEO nanostructures developed on the surface of droplets after solvent annealing. (e) A scheme of cross-sectional view of PS-*b*-PEO droplets with terraced structures after solvent annealing.

The thin concentric layer grown around the terraced droplet is another characteristic feature of our system and corresponds to brush monolayer of PS-*b*-PEO copolymer. The monolayered brush layer is ~7 nm in thickness in which polar PEO blocks are in contact with native oxide of Si substrate as shown in the schematic of Figure 5e. The wetting tendency of the brush monolayer on Si surface can be estimated by the spreading coefficient, S, which can be defined by $S = \gamma_{Si\ wafer/benzene} - \gamma_{PEO/Si\ wafer} - \gamma_{PS/benzene}$ in our system. Based on the interfacial surface tensions calculated by the harmonic mean equation with the values given in the literature as summarized in Table 1, S turned out a positive value of ~17.1 J/m^2, indicative of the stabilization of brush monolayer on a Si substrate.

The growth of brush monolayer was monitored as a function of solvent annealing time. As *as-transferred* dewetted droplets were exposed to a benzene vapor for 20 s, concentric wetting of the brush monolayer began at each droplet, as shown in Figure 6a. At the same time, the size of the *as-transferred* PS-*b*-PEO droplets increased gradually with solvent exposure time (Figure 6b,c). The brush layer exhibited slow, continuous growth with the dewetted droplet acting as a reservoir which feeds block copolymer molecules. As time progressed, the spherical-cap droplets were transformed into terraced ones arising from the formation of the

Table 1. Interfacial Surface Tension Values of the Materials Used in the Experiments

material A	material B	$\gamma_{AB}(\gamma^p + \gamma^d)$/ dyn cm^{-1}	γ^d/dyn cm^{-1}	γ^p/dyn cm^{-1}
Si wafer[a]	air	65.1	29.9	35.2
benzene[a]	air	29.2	28.5	0.6
PEO[a]	air	33.8	9.6	24.2
PS[a]	air	32.1	26.7	5.4
PDMS[a]	air	19.8	19	0.8
PS-*b*-PEO	air	25.2	19.4	5.8
Si wafer[b]	benzene	33.57		
PEO[b]	Si wafer	12.47		
PS[b]	benzene	3.99		

[a] Obtained from *Polymer Handbook* by J. Brandup, 4th ed. [b] Calculated from the harmonic mean equation

$$\gamma_{12} = \gamma_1 + \gamma_2 - \frac{4\gamma_1^d\gamma_2^d}{\gamma_1^d + \gamma_2^d} - \frac{4\gamma_1^p\gamma_2^p}{\gamma_1^p + \gamma_2^p}$$

where γ^p and γ^d are polar and disperse surface tension.

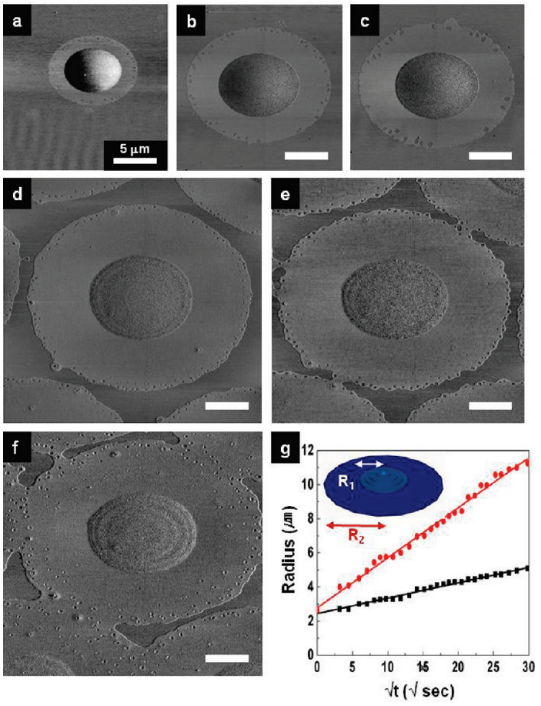

Figure 6. (a−f) AFM images of a dewetted PS-*b*-PEO droplet with the characteristic brush monolayer captured at different solvent annealing time: (a) 20, (b) 200, (c) 290, (d) 890, (e) 1130, (f) and 1370 s. (g) Plots of the radii of the terraced droplet and the circular brush monolayer as a function of solvent annealing time. Both plots show the linear relationship between root value of solvent annealing time and both the radii.

spherical PEO microdomains with the improved ordering. Further solvent annealing resulted in merging separate brush layers with each other (Figure 6e) and finally covered the entire Si substrate with the grown brush layer (Figure 6f). We examined the growth rates of both radii of brush monolayer and dewetted droplet, as defined in the scheme of Figure 5e. Interestingly, both radii increase linearly with $\sqrt{t}$ before concentric brush layers were in contact with each other, as shown in Figure 6g, which indicates that both radii grow pseudo-diffusively with the relation of $R(t) \sim (Dt)^{1/2}$, where D corresponds to a diffusion coefficient of the front. Spreading of symmetric block copolymer droplets above and below the order−disorder transition is recently developed by Croll et al.[37] The droplet in a disordered state grows as $R \sim t^m$, where t is time, with $m = 1/10$, consistent with Tanner's law. In contrast, a droplet in ordered state spread much more slowly with

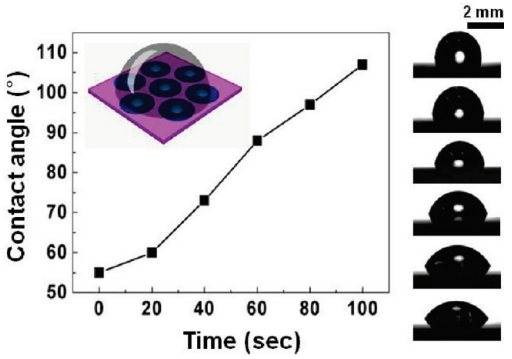

Figure 7. Plot of contact angle of a water droplet on micropatterned PS-*b*-PEO droplets transferred from 10 μm hexagonal PDMS prepattern as a function of solvent annealing time. The contact angle of ~55° on *as-transferred* pattern is varied to 105° after 100 s solvent annealing, as shown in photographs from bottom to top. A schematic not in scale shows a water droplet on the controlled micropattern of PS-*b*-PEO.

$m \sim 0.05 \pm 0.01$. In our case, as noted, we observed a diffusive growth of both brush layer and droplet with an exponent, $m \sim 0.5$, much faster than that of droplets thermally induced. The diffusive motion of our system may be attributed to solvent vapor, i.e., solvent precursor wetting layer.

In spite of universal behavior of the pseudo-diffusion of various monolayers including simple liquids,[20,38−40] smectic liquid crystal,[19] brush macromolecules,[41] and block copolymer,[42] the resulting structure of the droplet significantly depends in a complex way on the nature of the fluid and the layer grafted on top of the substrate. On pure substrates, the diffusion coefficient is proportional to the affinity of the liquid molecules for the solid surface and inversely to the friction of the fluid on the solid. The estimated diffusion coefficients of both brush and droplet layer are approximately 8.58×10^{-10} and 8.1×10^{-11} cm^2/s, respectively. In our system, the spread rate of the brush monolayer is ~10 times faster than that of the droplet.

Our micropatterning technique of block copolymer droplets combined with solvent annealing provides an efficient way to tune surface polarity of a substrate containing the patterned droplets as a function of solvent annealing time. For instance, the contact angle of a water droplet on an *as-transferred* micropattern of ~55° almost linearly increases with solvent annealing time, as shown in Figure 7. In this particular micropattern containing ~2 μm droplets (Figure 3a), solvent annealing for 100 s was long enough to cover whole Si wafer with brush monolayer grown from the individual droplets, resulting in a water contact angle of ~105°, which corresponds to that of a pure PS as shown in Figure 7. The controlled growth of brush monolayer with PS block pointing to air by solvent annealing, therefore, allows us to tune the contact angle of a water droplet in the range over 50°.

Conclusions

We precisely controlled the growth of brush monolayers of micropatterned arrays of hierarchically ordered block copolymer droplets on a Si substrate. Solvent vapor annealing rendered the brush monolayer with the thickness of ~7 nm concentrically spread around the individual PS-*b*-PEO droplets micropatterned and transferred from a topographic PDMS prepattern. The radius of the concentric brush monolayer turned out to grow proportional to $\sqrt{t}$. The characteristic terraced structure was developed upon solvent annealing, arising from highly ordered spherical PEO microdomains confined in the droplets. Our method allowed for the fabrication of patterned arrays of the multiterraced microdroplets, consisting of both brush monolayer and hierarchically ordered spherical microdomains over a large area. In turn, the control of both shape and microstructure of the

individual microdroplets with solvent annealing time enabled us to tune the contact angle of a water droplet in the range of 50°, offering a new way to develop polarity tailored surfaces.

Acknowledgment. This work was supported by DAPA and ADD, the Korea Research Foundation Grant funded by the Korean Government (MOEHRD; KRF-2005-042-D00110), and Seoul Research and Business Development Program (10701). Finally, this work was supported by the Second Stage of the Brain Korea 21 Project in 2006 and by the Seoul Science Fellowship. This work was supported by the National Research Foundation of Korea (NRF) grant funded by the Korea government (MEST) (No. 2009-0080235).

References and Notes

(1) Hamley, I. W. *Angew. Chem., Int. Ed.* **2003**, *42*, 1692.
(2) Park, C.; Yoon, J.; Thomas, E. L. *Polymer* **2003**, *44*, 6725.
(3) Hawker, C. J.; Russell, T. P. *MRS Bull.* **2005**, *30*, 952.
(4) Jeong, S.-J.; Kim, J. E.; Moon, H.-S.; Kim, B. H.; Kim, S. M.; Kim, J. B.; Kim, S. O. *Nano Lett.* **2009**, *9*, 2300.
(5) Kim, T. H.; Hwang, J.; Hwang, W. S.; Huh, J.; Kim, H.-C.; Kim, S. H.; Hong, J. M.; Thomas, E. L.; Park, C. *Adv. Mater.* **2008**, *20*, 522.
(6) Carvalho, B. L.; Thomas, E. L. *Phys. Rev. Lett.* **1994**, *73*, 3321.
(7) Croll, A. B.; Massa, M. V.; Matsen, M. W.; Dalnoki-Veress, K. *Phys. Rev. Lett.* **2006**, *97*, 204502.
(8) Kim, J. U.; Matsen, M. W. *Soft Matter* **2009**, *5*, 2889.
(9) Epps, T. H., III; DeLongchamp, D. M.; Fasolka, M. J.; Fischer, D. A.; Jablonski, E. L. *Langmuir* **2007**, *23*, 3355.
(10) Green, P. F. *J. Polym. Sci., Part B: Polym. Phys.* **2003**, *41*, 2219.
(11) de Gennes, P. G. *Rev. Mod. Phys.* **1985**, *57*, 827.
(12) Adamson, A. W. *Physical Chemistry of Surfaces*, 4th ed.; Wiley: New York, 1982.
(13) Cazabat, A. M. *Contemp. Phys.* **1987**, *28*, 347.
(14) Leger, L.; Joanny, J. F. *Rep. Prog. Phys.* **1992**, *55*, 431.
(15) Ma, X.; Gui, J.; Smoliar, L.; Grannen, K.; Marchon, B.; Bauer, C. L.; Jhon, M. S. *Phys. Rev. E* **1999**, *59*, 722.
(16) De Coninck, J.; D'Ortona, U.; Koplik, J.; Banavar, J. R. *Phys. Rev. Lett.* **1995**, *74*, 928.
(17) Betelú, S.; Law, B. M.; Huang, C. C. *Phys. Rev. E* **1999**, *59*, 6699.
(18) De Coninck, J.; Fraysse, N.; Valignat, M. P.; Cazabat, A. M. *Langmuir* **1993**, *9*, 1906.
(19) Lucht, R.; Bahr, Ch. *Phys. Rev. Lett.* **2000**, *85*, 4080.
(20) Heslot, F.; Fraysse, N.; Cazabat, A. M. *Nature* **1989**, *338*, 640.
(21) Xu, L.; Salmeron, M.; Bardon, S. *Phys. Rev. Lett.* **2000**, *84*, 1519.
(22) Tang, M.; Hong, M. H.; Choo, Y. S. *2008 IEEE PhotonicsGlobal at Singapore, IPGC* **2008**, 4781512.
(23) Péres, L. O.; Gruber, J. *Mater. Sci. Eng. C* **2007**, *27*, 67.
(24) Wu, M.-H.; Park, C.; Whitesides, G. M. *Langmuir* **2002**, *18*, 9312.
(25) Lu, Y.; Yin, Y.; Xia, Y. *Adv. Mater.* **2001**, *13*, 34.
(26) Kim, S. H.; Misner, M. J.; Xu, T.; Kimura, M.; Russell, T. P. *Adv. Mater.* **2004**, *16*, 226.
(27) Kim, S. H.; Misner, M. J.; Russell, T. P. *Adv. Mater.* **2004**, *16*, 2119.
(28) Park, S.; Dong, H. L.; Xu, J.; Kim, B.; Sung, W. H.; Jeong, U.; Xu, T.; Russell, T. P. *Science* **2009**, *323*, 1030.
(29) Kim, T. H.; Huh, J.; Hwang, J.; Kim, H.-C.; Kim, S. H.; Sohn, B.-H.; Park, C. *Macromolecules* **2009**, *42*, 6688.
(30) Yoon, B. K.; Huh, J.; Kim, H.-C.; Hong, J.-M.; Park, C. *Macromolecules* **2006**, *39*, 901.
(31) Lee, G.; Jo, P. S.; Yoon, B.; Kim, T. H.; Acharya, H.; Ito, H.; Kim, H.-C.; Huh, J.; Park, C. *Macromolecules* **2008**, *41*, 9290.
(32) Hirasawa, S.; Saito, Y.; Nezu, H.; Ohashi, N.; Maruyama, H. *IEEE Trans. Semi. Manuf.* **1997**, *10*, 438.
(33) Wu, S. *Polymer Interface and Adhesion*; Marcel Dekker: New York, 1982; Chapter 5.
(34) Kim, H.; Yoon, B.; Sung, J.; Choi, D.-G.; Park, C. *J. Mater. Chem.* **2008**, *18*, 3489.
(35) Tang, C.; Bang, J.; Stein, G. E.; Fredrickson, G. H.; Hawker, C. J.; Kramer, E. J.; Sprung, M.; Wang, J. *Macromolecules* **2007**, *40*, 2453.
(36) Stein, G. E.; Kramer, E. J.; Li, X.; Wang, J. *Macromolecules* **2008**, *41*, 4328.
(37) Croll, A. B.; Dalnoki-Veress, K. *Eur. Phys. J. E* **2009**, *29*, 239.
(38) Heslot, F.; Cazabat, A. M.; Levinson, P. *Phys. Rev. Lett.* **1989**, *62*, 1286.
(39) Heslot, F.; Fraysse, N.; Cazabat, A. M.; Levinson, P.; Carles, P. In *Wetting Phenomena*; De Coninck, J., Dunlop, F., Eds.; Springer-Verlag: Berlin, 1989.
(40) De Coninck, J.; Hoorelbeke, S.; Valignat, M. P.; Cazabat, A. M. *Phys. Rev. E* **1993**, *48*, 4549.
(41) Xu, H.; Shirvanyants, D.; Beers, K.; Matyjaszewshi, K.; Rubinstein, M.; Sheiko, S. S. *Phys. Rev. Lett.* **2004**, *93*, 206103.
(42) Belyi, V. A.; Witten, T. A. *J. Chem. Phys.* **2004**, *120*, 5476.